*Journal of Engineering Physics and Thermophysics, Vol. 76, No. 2, 2003*

# COMPUTATIONAL MODELING OF THE OPTICAL PUMPING OF SOLID-STATE LASERS AND THE HEATING OF THE ACTIVE ELEMENT WITH ALLOWANCE FOR WATER COOLING

**A. V. Kondrashenko, V. M. Linnik, A. G. Sirotkina, and V. D. Urlin**

UDC 621.373.826

*Two-dimensional nonstationary models of optical pumping of a solid-state laser in the presence of a reflector and heating of a cylindrical or plane active element with water cooling have been described. The results of calculations of the space-time dependence of the pumping rate and the temperature in the active element have been given for different versions of a neodymium laser with a crystalline active medium in laser-diode pumping.*

**Introduction.** Glass and crystalline lasers stand out at present as having a range of properties determining their wide use. They have been the focus of a great many works, including computational-theoretical ones (see [1, 2] and the references therein). The space-time distribution of the pumping rate and the temperature in the active element (AE) are the main indices of a solid-state laser. They largely determine the radiative characteristics of high-power solid-state lasers: the shape of a laser pulse, the output power and the efficiency, and the divergence and spectral width of the laser line. Therefore, prediction and description of these quantities and optimization of the parameters of solid-state lasers necessitate creation of the corresponding computational-theoretical models. In the general case this is a difficult problem, especially when one uses cross-pumped lasers, where the space distributions of the pumping rate and the temperature in the active element depend on many factors.

**Model of Optical Pumping of a Solid-State Laser.** The rate of change of the population of the energy level of pumping of the activator ions in the active element of a solid-state laser is described by the following equation:

$$\frac{\partial N_{\mathrm{p}}(\mathbf{r}, t)}{\partial t} = N_0(\mathbf{r}, t) \int_{\omega_1}^{\omega_2} \sigma(\omega, T)\, \Phi(\mathbf{r}, t, \omega)\, d\omega\,, \tag{1}$$

where the spectral intensity of pumping radiation is

$$\Phi(\mathbf{r}, t, \omega) = \int_{4\pi} \chi(\omega, \mathbf{l})\, Q_0(t, \omega, \mathbf{l}) \exp\left[-\sigma(\omega, T) \int_0^{s(r)} n(\mathbf{r}', t)\, ds\right] d\Omega\,. \tag{2}$$

Integration in (2) is carried out from a given point $A$ inside the active element with respect to the solid angle $4\pi$ (Fig. 1). An analogous approach was used in the computational model of a photodissociation iodine laser [3–5]. Solid-state lasers, unlike the indicated one, can have pumping sources with an arbitrary indicatrix of radiation and a complex spectral characteristic. The presence of the delivering and focusing optics also complicates the modeling of solid-state lasers. For the case of a cylindrical active element surrounded by symmetrically arranged pumping sources of finite length, Eq. (1) in spherical coordinates acquires the form

$$\frac{\partial N_{\mathrm{p}}(\mathbf{r}, \varphi, t)}{\partial t} = N_0(r, \varphi, t) \int_{\omega_1}^{\omega_2} \sigma(\omega, T)\, Q_0(t, \omega) \sum_1^J \int_0^{\psi_j} f(\alpha)\, (F_{1j} + F_{2j})\, d\psi\, d\omega\,, \tag{3}$$

Institute of Laser-Physical Research, Russian Federal Nuclear Center–All-Russia Scientific-Research Institute of Experimental Physics, Sarov, Russia; email: linnik@otd13.vniief.ru. Translated from Inzhenerno-Fizicheskii Zhurnal, Vol. 76, No. 2, pp. 72–79, March–April, 2003. Original article submitted August 21, 2002.

 1062-0125/03/7602-0316$25.00 

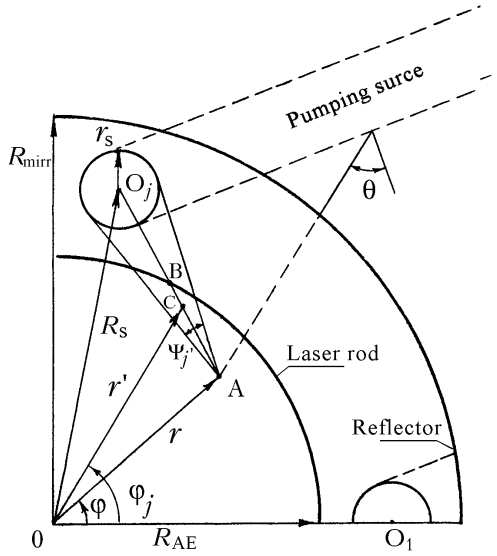

Fig. 1. Cross section of the pumping block.

where

$$F_{nj} = \int_0^{\theta_{nj}} \chi(\omega, \varphi, \theta)\, f(\theta) \sin\theta \exp[-g(r, \varphi, t)/\cos\theta]\, d\theta\,; \tag{4}$$

$$g(r, \varphi, t) = \sigma(\omega, T) \int_0^{a_j(r,\varphi)} N_0(r_j', \varphi_j, t)\, ds\,; \tag{5}$$

$$a_j(r, \varphi) = \mathrm{AB} = r_j - \sqrt{R_{AE}^2 - R_s^2 k_j^2} - R_s\sqrt{1 - 2k_j^2}\,; \tag{6}$$

$$r_j(r, \varphi) = \mathrm{AO}_j = \sqrt{R_s^2 + r^2 - 2R_s r\cos\gamma}\,, \quad k_j(r, \varphi) = (r/r_j)\sin\gamma\,, \quad \gamma = [2\pi(j-1)/J] - \varphi\,;$$

$$r_j'(r, \varphi) = \mathrm{OC} = \sqrt{(a-s)^2 + r^2 - 2(a-s)\sqrt{r^2 - R_s^2 k_j^2}}\,, \quad \varphi_j(r, \varphi) = \varphi + \arcsin\left[\frac{R_s(a-s)k_j}{r_j' r}\right], \quad s = \mathrm{BC}\,.$$

The finite length of the source is allowed for by the values of the limits of integration with respect to the angle $\theta_n = \arctan[L_n/(r_j - r_s)]$. In the presence of a diffuse reflector in the pumping module, it is assumed that the reflector surface is an additional isotropically radiating source with an intensity of $Q_1 = Q(R_{mirr}, \omega, t)\, K(\omega)/2\pi$. We can analogously take account of any subsequent $q$th reflection: $Q_q = Q_{q-1}(R_{mirr}, \omega, t)\, K(\omega)/2\pi$.

To allow for the contribution of the reflector we must replace the quantity $Q_0$ in Eqs. (2) and (3) by the sum $Q_0 + \Sigma Q_i$. Heat release in the working medium of a solid-state laser is attributed to the transformation of a part of the absorbed energy of pumping light to heat. Therefore, solution of Eqs. (1) and (3) enables us to determine, in addition to the pumping rate, the space-time function of heat release required for calculation of the temperature field in the active element.

**Thermal Model of the Active Element of a Solid-State Laser with Liquid Cooling.** Nonuniform heating in the working medium of a solid-state laser causes thermomechanical stresses and strains, additional population of the lower laser level, and a nonuniform change in the refractive index [6–9]. To determine the space-time dependence of the temperature in the cylindrical active element we have used the heat-conduction equation in a polar coordinate system [10]

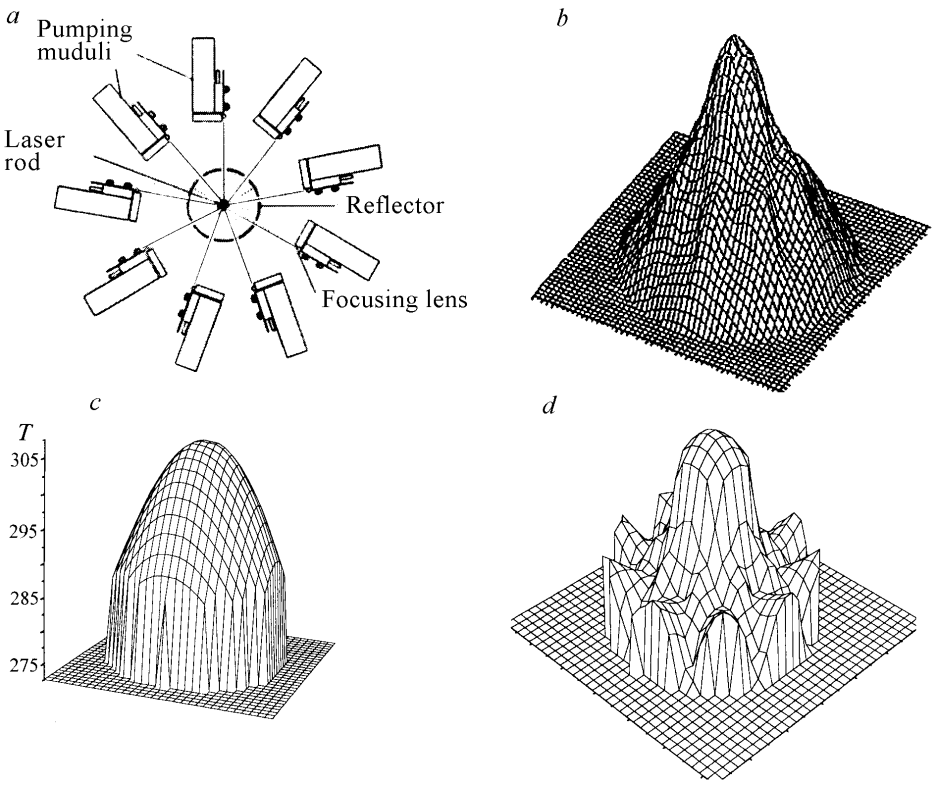


Fig. 2. Computational modeling of the diode-pumped solid-state laser from [11] (Nd–YAG active element, ∅ 5 mm, $N_{Nd} = 12.4 \cdot 10^{19}$ cm$^{-3}$; $\lambda_{max} = 808$ nm, and $\Delta\lambda = 4$ nm): a) scheme of the pumping block, b and d) qualitative distribution of the pumping rate in the cross section of the active element in experiment and in calculation; c) calculated temperature profile of the active element at the instant of time $t = 4$ sec. $T$, K.

$$\frac{\rho c}{q}\frac{\partial T(r,\varphi,t)}{\partial t} = \frac{1}{r}\frac{\partial}{\partial r}\left[r\frac{\partial T(r,\varphi,t)}{\partial r}\right] + \frac{1}{r^2}\frac{\partial^2 T(r,\varphi,t)}{\partial \varphi^2} + \frac{1}{q}G(r,\varphi,t) \tag{7}$$

with the boundary condition $\partial T/\partial\varphi = 0$ at $\varphi = 0$ and $\varphi = 2\pi/J$, where the rate of volume heat release is

$$G(r,\varphi,t) = \int_{\omega_1}^{\omega_2} A(\omega)\,\hbar\omega\,\frac{\partial N_p(r,\varphi,t)}{\partial t}\,d\omega\,, \tag{8}$$

the function $\partial N_p/\partial t$ being found from Eq. (1). When the cooling of the active-element surface by a liquid flow is allowed for, we add another boundary condition:

$$\frac{\partial T}{\partial r} = -\frac{h}{q}\left[T(r,\varphi,t) - T_{liq}\right] \quad \text{for} \quad r = R_{AE}\,. \tag{9}$$

Based on the above models, we created a PSL two-dimensional nonstationary computer program. The numerical procedures developed for simultaneous solution of the equations of transfer of pumping radiation and of heat conduction in the active element are described in the Appendix. Heating of the active element leads to optical distortions in it, which are associated mainly with photoelastic and temperature changes in the refractive index. The temperature changes have a dependence on the coordinates and time common to the active-element temperature:

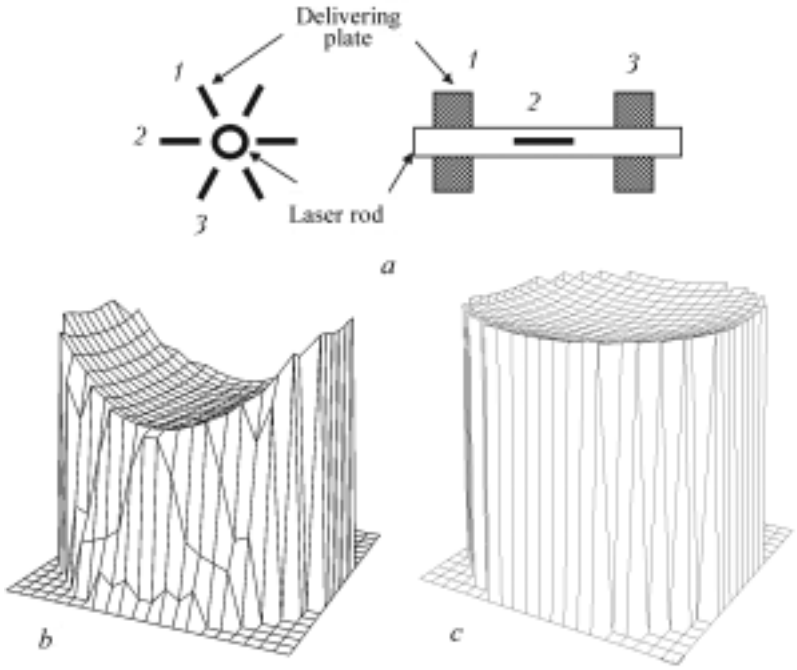


Fig. 3. Calculations of the pumping rate of the diode-pumped solid-state laser from [15] (Nd–YAG active element, ∅ 4 mm, $N_{Nd} = 8.22 \cdot 10^{19}$ cm$^{-3}$; $\lambda_{max}$ = 804.4 nm, and $\Delta\lambda$ = 3 nm): a) scheme of the pumping block [1–3) pumping modules]; b and c) $N_p$, profiles in the actual structure and in the hypothetical structure in irradiation on six sides.

$$\Delta n_T(r, \varphi, t) = \frac{\partial n}{\partial T} \Delta T(r, \varphi, t) . \tag{10}$$

Consequently, the PSL program enables us to calculate the space-time dependence of the temperature component of the change in the refractive index in the working medium of the solid-state laser.

**Computational Modeling of Diode-Pumped Crystalline Lasers.** Here we consider specific specimens of high-power solid-state crystalline lasers with diode pumping.

*German Version of the Laser*. Production prototypes of diode-pumped solid-state lasers are being actively developed in Germany [11–13]. Creation of a quasicontinuous laser with a power of $P_{las.r}$ = 750 W and an optical-laser efficiency of 40% is reported in [12]. Of interest is [11], where almost all the initial data required for computational modeling are given except for the data on the indicatrix of radiation at the output of the focusing lens. In this work, the water-cooled yttrium-aluminum-garnet active element with neodymium (Nd) ions as the activator (Nd–YAG) with $N_{Nd} = 1.24 \cdot 10^{20}$ cm$^{-3}$, $L$ = 22 cm, and ∅ = 0.5 cm was surrounded by a diffuse reflector with nine longitudinal cuts for introduction of pumping radiation (Fig. 2a). As the pumping sources, we used 108 linear arrays of laser diodes with $P_{las.r}$ = 10 W each, $\lambda_{max}$ = 808 nm and $\Delta\lambda$ = 4 nm. The linear arrays of laser diodes were arranged into 18 modules; the radiation of each module was focused to the laser rod by a cylindrical lens. All these data were built into the calculations according to the PSL program. It was assumed that the temperature of running water remains constant and is equal to $T_{liq}$ = 283 K. The calculation results are presented in Fig. 2b–d. A substantial nonuniformity of the angular distribution of the pumping rate in the surface layer of the active element is noteworthy. In the experiment of [11], this effect was weak. This suggests that the indicatrix of pumping radiation at the output of the focusing lens built into the calculations differed from the actual indicatrix. The edge effects associated with the finiteness of the length of the pumping sources turned out to be insignificant. The temperature profile $T(r, \varphi)$ established after $t$ = 4 sec was angularly uniform, just as in the calculations of [11]. The calculated values of the temperature difference between the axis and the surface of the active element turned out to be close: $\Delta T = 20^o$ in the present work and $21^o$ in [11]. Despite the heat release being nonuniform over the radius, the calculated profile of the temperature differs little from

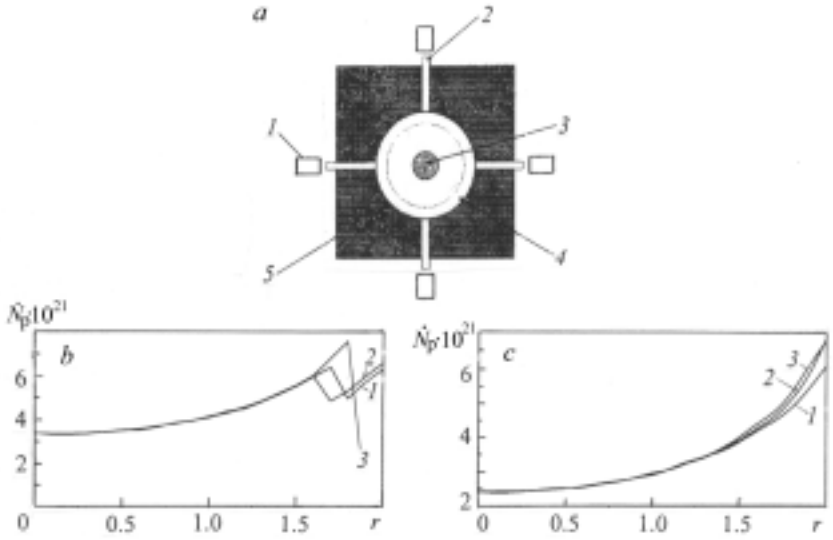


Fig. 4. Calculations of the pumping rate of the diode-pumped solid-state laser from [16] (Nd–YAG active element, ∅ 4 mm, $N_{Nd} = 13.7 \cdot 10^{19}$ cm$^{-3}$; $\lambda_{max}$ = 808 nm, and $\Delta\lambda$ = 3 nm): a) scheme of the pumping block [1) linear arrays of laser diodes; 2) glass plate; 3) laser rod; 4) glass tube; 5) diffuse reflector); b and c) radial dependence of $N_p$ for different values of the angle φ for the gap between the active element and the plate $\Delta r$ = 4 and 6 mm [1) $\varphi = 0^o$, 2) $22^o$, and 3) $45^o$]. *r*, mm; $\dot{N}_p$, cm$^{-3}$·sec$^{-1}$).

a parabolic profile. This enables us to apply formulas derived for a lenticular medium [2, 14]. Thus, the calculation of the focal length of a thermal lens without allowance for the curvature of the active-element ends and photoelastic effects yielded $f_{lens}$ = 13.5 cm (for a source length of 16 cm and $\partial n/\partial T = 7.3 \cdot 10^{-6}$ K$^{-1}$ from [11]). The close value $f_{lens}$ = 15 cm was recorded in the experiment of [11]. This suggests that in this case the contribution of the temperature change of the refractive index to the formation of the thermal lens turned out to be determining.

*Japanese Version of the Laser*. The original quasicontinuous laser with diode pumping has been described in [15]. Its characteristic properties are its simplicity of structure and the absence of focusing optics. A scheme of the pumping block is presented in Fig. 3. The laser rod from an Nd–YAG crystal with $N_{Nd} = 8.22 \cdot 10^{19}$ cm$^{-3}$, *L* = 11.5 cm, and ∅ = 4 mm surrounded by a diffuse reflector was cooled by running water. To deliver pumping light to the water-cooled tube use was made of thin glass plates with a thickness of 0.5 mm as the light guides. The plates were put into the reflector slots. There were no optical elements between the pumping source and a plate. The pumping block consisted of three modules arranged along the laser axis. Each module incorporated two linear arrays of laser diodes with a specific radiation power of 20 W/cm symmetrically arranged about the active element and two delivering plates, which were rotated by an angle of $60^o$ about the axis relative to the neighboring pair of plates (Fig. 3a). Thus, each third of the active element was irradiated on both sides. In the case where the radiation line of the laser diode was shifted by 4.1 nm ($\lambda_{max}$ = 804.4 mm) from the principal absorption line of Nd–YAG, the intensity profile of spontaneous radiation measured by Kojima et al. [15] at the output of the excited active element turned out to be uniform, in practice. This led them to the conclusion that the pumping distribution is uniform in the active element. However our calculation revealed a substantial radial and angular nonuniformity of the pumping rate (Fig. 3b). This was to be expected in irradiation of each third of the active element on both sides. For six sources symmetrically arranged about the active element, conversely, the calculation yielded a uniform distribution (Fig. 3c). It is precisely this case that corresponds to the experiment in which each of the six sources (two in each block) made the same contribution to the distribution of the spontaneous radiation at the output of the active element. The structure of the above-described laser was improved in [16]. In it, the laser rod was irradiated on four sides throughout the length (Fig. 4). The linear arrays of laser diodes were arranged lengthwise in line. The radiation line of the laser diodes had $\lambda_{max}$ = 808 nm for $\Delta\lambda$ = 3 nm. Konno et al. [16] state that the laser pumping was uniform over the cross section. To check this we carried out calculations according to the PSL program. In addition to the above characteristics, it was assumed

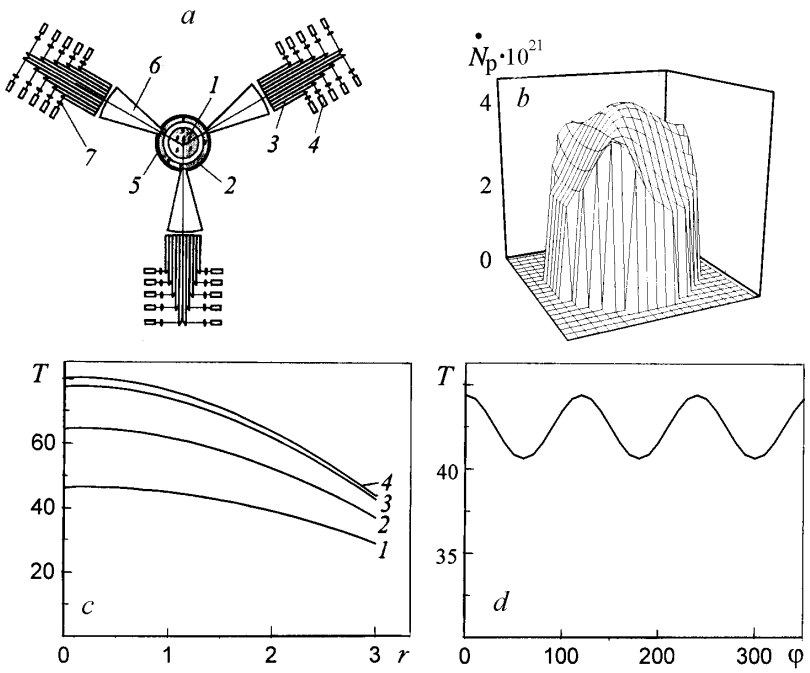


Fig. 5. Calculations of the pumping rate and the temperature of the active element of a kW quasicontinuous solid-state laser with diode pumping: a) scheme of the pumping block [1) active element; 2) cooling tube; 3) light-delivering plate; 4) linear array of laser diodes; 5) reflecting coating, 6) prismatic focuser; 7) cylindrical lens]; b) distribution of $\dot{N}_p$ in the cross section of the active element; c) radial distribution of $T$ at different instants of time after the beginning of pumping [1) $t$ = 0.5; 2) 1; 3) 2; 4) 3 sec]; d) steady-state angular distribution of $T$ on the active-element surface. $\dot{N}_p$, $cm^{-3} \cdot sec^{-1}$; $r$, mm; $T$, $^oC$.

that the distance between the active-element surface and the delivering plate is $\Delta r$ = 2 nm, while the radiation at exit from the plate has a Gaussian distribution with $\theta_\perp = 36^o$. It turned out as a result of the calculation that the nonuniformity of the pumping-rate distribution was much lower than in [15] at $\lambda_{max}$ = 804.4 nm. But a substantial angular nonuniformity of pumping in the surface layer persisted. The degree of this nonuniformity depends on the distance between the active element and the plate $\Delta r$ (Fig. 4). Whereas at $\Delta r \le 4$ mm we observe shadow regions into which direct pumping radiation finds no way, at $\Delta r$ = 6 mm the curves of the radial distribution of the pumping rate in the active element with different values of the angle φ coincide, in practice. The laser from [16] possesses a number of advantages. Konno et al. [16] were able to obtain the power $P_{las.r}$ = 80 W in the case of an electrical efficiency of 8% and a good quality of the beam in the single-mode regime. Such a structure can be considered as a nominee for the module of a high-power technological laser.

*Kilowatt Laser*. We participated in developing a quasicontinuous kilowatt (kW) solid-state laser with diode pumping within the framework of a project (No. 377) of the International Science and Technology Center. A scheme of the pumping block of one proposed version is presented in Fig. 5a. The radiation of the linear arrays of laser diodes 4 with a specific power of 10 W/cm is introduced into a pile of light-delivering plates 3 via cylindrical microlenses 7. In the plates, pumping-radiation beams are totally internally reflected on the slopes of the plates and they are rotated by an angle of $90^o$. A 19-mm-wide radiation beam formed in this manner is guided to the inlet of the prismatic focuser 6, which decreases its width to 1 mm at the outlet. The conditions of calculation of the pumping and heating of the active element were as follows: the cylindrical Nd–YAG active element with a concentration of $N_{Nd} = 1.14 \cdot 10^{20}$ $cm^{-3}$, $L$ = 13 cm, and ∅ = 6.3 mm surrounded by a diffuse reflector was cooled by running water at $T_{liq}$ = 283 K. The total number of linear arrays of laser diodes was 270 (90 per focuser) with a specific radiation power of 10 W/cm with a Gaussian indicatrix, $\theta_\perp = 15^o$, $\lambda_{max}$ = 808 nm, and $\Delta\lambda$ = 6 nm. The results of calculating the two-dimensional distribution of the pumping rate in the active element and the space-time dependence of the tempera-

ture are presented in Fig. 5b–d. It is seen that in irradiation on three sides we observe the angular nonuniformity not only of the pumping rate but also of the temperature in the surface layer of the active element, although the temperature difference is no higher than $3^o$. The calculations yield that the stationary temperature field is established within 4 sec after the beginning of pumping. We have $T$ = 353 K on the axis of the laser rod and 310 to 313 K on the surface depending on the angle $\varphi$. In the calculation with five focusers, in irradiating the active element on five sides, the distributions of the pumping rate and the temperature turned out to be independent of the angle. The analysis has shown that in both versions the radial dependence of the temperature is nearly parabolic. This enables us to use the expressions derived for a quadratic medium and characterizing a thermal lens and to apply a spherical lens to compensate for the focusing of laser radiation.

## CONCLUSIONS

We have created a two-dimensional model of pumping and heating of the active element of a solid-state laser. We have developed numerical procedures for simultaneous solution of the equations of transfer of pumping radiation and heat conduction in the active element of a solid-state laser with allowance for water cooling which have been used as the basis for the PSL computer program. This program makes it possible to calculate the space-time dependence of the pumping rate, the heat release, and the temperature and the temperature component of the change in the refractive index in the active element having the shape of a cylinder of finite length or a plate in the presence of a diffuse reflector. Pulsed or continuous pumping sources may have arbitrary dependences of the radiation intensity on the time, the wavelength, and the angle of propagation.

In modeling the German version of a diode-pumped solid-state laser with a cylindrical active element, we have revealed satisfactory agreement of the calculated results of the present work with the results obtained by the developers of the laser. It has been established that the time in which the distribution of the temperature in the active element reaches its steady-state value is 4 sec.

The computational analysis of the Japanese version of a rod diode-pumped solid-state laser with delivering plates and the absence of focusing optics leads us to the conclusion that the idea (expressed by the developers of the laser) of the spatial uniformity of pumping of the active element is incorrect. In the modified version, a substantial dependence of the pumping-rate distribution on the gap between the active element and the delivering plate has been revealed.

The computational prediction of the characteristics of laser radiation and optimization of the parameters of the pumping block carried out with our participation resulted in an acceptable version of a kW continuous solid-state laser with diode pumping.

This work was carried out under project No. 377 of the International Science and Technology Center. The authors of the paper express their thanks to V. A. Volkov, G. M. Mishchenko, and V. M. Romanov for useful discussions of the materials presented.

## APPENDIX

In numerical solution of Eq. (3), the concentration of unexcited activator ions at each time step at each point of the space grid is calculated according to a scheme of the form [3]

$$(N_0)_{ik}^{m+1} = (N_0)_{ik}^{m} (1 - 0.5\tau W_{ik}^{m}) / (1 + 0.5\tau W_{ik}^{m}) , \tag{A1}$$

$$i = 1, 2, ..., I ; \quad k = 1, 2, ..., K ;$$

$$W_{ik}^{m} = \int_{\omega_1}^{\omega_2} \sigma (\omega, T_{ik}^{m}) Q_0 (\omega, t_m + \tau/2) \sum_{1}^{J} \int_{0}^{\psi_j} f (\alpha) (F_{1j} + F_{2j}) \, d\psi \, d\omega , \tag{A2}$$

the functions $F_{nj}$ being determined by relations (4)–(6). To calculate the integral with respect to $s$ in (5) use is made of the Simpson method of fourth order. In (A2), in accordance with the integral theorem of $\psi$ average over the angle

we use the values of the concentrations $N_0(t_m, r_l, \varphi_l)$ taken from the beam **1** which connects the center of the $j$th source with a given point A. For numerical integration of the heat-conduction equation (7) we use the five-point difference scheme of variable directions of the form [10]

$$\frac{\rho c}{q\tau}(T_{ik} - T_{ik}^m) = \Lambda_\varphi(T_{ik}), \quad \frac{\rho c}{q\tau}(T_{ik}^{m+1} - T_{ik}) = \Lambda_r(T_{ik}^{m+1}) + \frac{G_{ik}}{q}, \tag{A3}$$

$$\Lambda_\varphi(T_{ik}) = \frac{2}{r_k^2(\Delta\varphi_{i+0.5} + \Delta\varphi_{i-0.5})}\left[\frac{T_{i+1k} - T_{ik}}{\Delta\varphi_{i+0.5}} - \frac{T_{ik} - T_{i-1k}}{\Delta\varphi_{i-0.5}}\right], \tag{A4}$$

$$\Lambda_r(T_{ik}) = \frac{2}{\Delta r_{k+0.5} + \Delta r_{k-0.5}}\left[r_{k+0.5}\frac{T_{ik+1} - T_{ik}}{\Delta r_{k+0.5}} - r_{k-0.5}\frac{T_{ik} - T_{ik-1}}{\Delta r_{k-0.5}}\right], \tag{A5}$$

$$i = 2, 3, ..., (I-1); \quad k = 2, 3, ..., (K-1).$$

For $I(K-1)+1$ unknown $T_{ik}$ there are $(I-2)(K-2)$ equations of the form (A3)–(A5) for the internal points of the grid. Additional $2(K-2)$ relations for the solution of the first stage of the scheme (Eqs. (A3) and (A4)) are obtained in approximation of the boundary condition $\partial T/\partial\varphi = 0$ for $\varphi = 0$ and $\varphi = 2\pi/J$:

$$(T_{Ik} - T_{I-1k})/\Delta\varphi_{I-0.5} = 0, \quad (T_{2k} - T_{1k})/\Delta\varphi_{3/2} = 0, \quad k = 2, 3, ..., (K-1). \tag{A6}$$

To solve the second stage of the scheme (Eqs. (A3)) and (A5) we take additional $(I-2)$ grid relations resulting from approximation of boundary condition (9) at the circular boundary of the computational region:

$$\frac{T_{iK}^{m+1} - T_{iK-1}^{m+1}}{\Delta r_{K-0.5}} = \frac{h}{q}[T_{\text{liq}} - T_{ik}], \quad i = 2, 3, ..., (I-1). \tag{A7}$$

We find the last lacking relation for closing the system of grid equations (A3) and (A5), approximating Eq. (7) with the use of the expression for the divergence in the vicinity of the point $r = 0$ [10]:

$$\text{div}\,[\text{grad}\,(T)] = \frac{1}{\pi r^2}\lim\int_0^{2\pi}(\partial T/\partial r)\,r d\varphi. \tag{A8}$$

Replacing the integral in (A8) by a sum and the integrand by differences, we can approximate Eq. (7) in the vicinity of the point $r = 0$ as follows [10]:

$$\rho c\,(T_1^{m+1} - T_1)/\tau = \frac{2qJ}{\pi\Delta r_{3/2}^2}\sum_{i=1}^{I-1}(T_{i2}^{m+1} - T_1^{m+1})\,\Delta\varphi_{i+0.5} + G. \tag{A9}$$

In (A9), subscript 1 denotes the grid point $r_1 = 0$ and it is taken into account that the $\varphi$ grid covers only the sector with an angle $2\pi/J$. For economical implementation of the first stage of the scheme in question (system (A3)–(A4) with circular boundary conditions (A6) for each value of $r_k$, $k = 2, 3, ..., K-1$) we carry out $\varphi$ running along the boundary of the corresponding sector [10]. As a result we obtain $I(K-2)$ values of $T_{ik}$, $i = 1, 2, ... I$ and $k = 2, 3, ..., K-1$. For the second stage of the scheme we first carry out direct running through all the internal radii of the grid beginning with the circular boundary. Upon the addition of Eq. (A9) and two boundary relations (A6) to $(I-2)$ trial relations of the form $T_{i2}^{m+1} = \alpha_{i2}T_{i1}^{m+1} + \beta_{i2}$, $i = 2, 3, ..., I-1$, we calculate the value of $T_1^{m+1}$ for $k = 2$. Thereafter,

carrying out inverse running through all the internal radii of the grid, we calculate all the values of $T_{ik}^{m+1}$ for $i$ = 2, 3, ..., $I-1$ and $k$ = 2, 3, ..., $K$. The calculation of the next step is completed by computation of the values of $T_{1K}^{m+1}$ and $T_{IK}^{m+1}$ from relations (A6) when $k = K$.

## NOTATION

$N_p$, population of the combined energy level of pumping of the activator ions; $N_p = \partial N_p/\partial t$, pumping rate; $N_0$, population of the ground level; $\omega = 2\pi\nu$, angular frequency of radiation; $\hbar\omega$, light-quantum energy; $T(r, \varphi, t)$, temperature of the active element; $\sigma(\omega, T)$, absorption cross section of the pumping light in the active element; $\mathbf{\Phi}(\mathbf{r}, t, \omega)$, spectral intensity of pumping radiation at a given space point of the active element; $Q_0$, spectral intensity of the radiation of the pumping source per unit solid angle in the direction of vector **1** lying on the straight line $O_jA$; $\chi(\omega, \mathbf{1})$, coefficient of attenuation of pumping radiation on the length from the source to the surface of the active element which allows for absorption, reflection, and refraction in the elements of delivering and focusing optics; $s$, path of the pumping-radiation quantum from the surface of the active element to the point in question; $J$, number of pumping sources; $\psi_j$, angle at which the $j$th source is seen in the cross section from a given point A; $L_n(n = 1, 2)$, distances from the ends of the source to the cross section in which point A lies; $r_s$, $R_{AE}$, and $R_{mirr}$, radii of the cylindrical source, the active element, and the mirror (reflector); $R_s$, distance between the axes of the source and the active element; $f(\alpha)$ and $f(\theta)$, functions (normalized to unity) characterizing the indicatrix of radiation of the sources; $\alpha$, angle $0O_jA$ (see Fig. 1); $Q(R_{mirr}, \omega, t)$, spectral intensity of the radiation from all the sources with allowance for their mutual shading that has reached the surface of the mirror with radius $R_{mirr}$; $K(\omega)$, coefficient of diffuse reflection of the mirror; $\rho$, $c$, and $q$, density, heat capacity, and thermal conductivity of the active element; $A(\omega)$, fraction of the energy of the absorbed light quantum going into heating; $h$, coefficient of heat exchange between the active element and the liquid; $T_{liq}$, liquid temperature; $\Delta n_T$, temperature component of the change in the refractive index; $\partial n/\partial T$, thermooptical coefficient; $P_{las.r}$, laser-radiation power; $N_{Nd}$, concentration of neodymium ions; $L$ and $\varnothing$, length and diameter of the active element; $\lambda_{max}$, wavelength at the maximum of the laser line; $\Delta\lambda$, width of the laser line at half-height; $f_{lens}$, focal length of the thermal lens; $\theta_\perp$, transverse divergence of the radiation beam at half-height; $\tau$, time step; $I$ and $K$, number of angular and radial calculation points; $W_{ik}^m$, probability of optical excitation of the activator ion; $\Lambda_\varphi(T_{ik})$ and $\Lambda_r(T_{ik})$, difference operators of second order in $\varphi$ and $r$. Subscripts: $i$ and $k$, space grids (in $\varphi$ and $r$); $m$, time grids; liq, liquid; mirr, mirror; s, source; $j$, number of the source; lens, lens; las.r, laser radiation (emission); max, maximum; p, pumping; $q$, number of reflection; AE, active element; Nd, neodymium.

## REFERENCES


1. A. A. Mak, L. N. Soms, V. A. Fromzel', and V. E. Yashin, *Neodymium-Glass Lasers* [in Russian], Moscow (1990).
2. G. M. Zverev and Yu. D. Golyaev, *Crystalline Lasers and Their Application* [in Russian], Moscow (1994).
3. V. D. Urlin, V. M. Linnik, and A. V. Kondrashenko, *Kvantovaya Elektron.*, **19**, No. 12, 1176–1181 (1992).
4. G. N. Vinokurov, V. Yu. Zalesskii, and P. I. Krepostnov, *Kvantovaya Elektron.*, **7**, No. 5, 944–956 (1980).
5. J. S. Cohen and O. P. Judd, *J. Appl. Phys.*, **55**, 2659–2671 (1984).
6. G. D. Baldwin and E. P. Reidel, *J. Appl. Phys.*, **38**, 2726–2738 (1967).
7. L. M. Osterink and J. D. Foster, *Appl. Phys. Lett.*, **12**, 128–131 (1968).
8. J. D. Foster and L. M. Osterink, *J. Appl. Phys.*, **41**, 3656–3663 (1970).
9. W. Koechner, *Appl. Opt.*, **9**, 2548–2553 (1970).
10. A. N. Tikhonov and A. A. Samarskii, *Equations of Mathematical Physics* [in Russian], Moscow (1977).
11. D. Golla, S. Knoke, W. Schone, G. Ernst, A. Tunnermann, and H. Welling, *Proc. SPIE*, **2379**, 120–128 (1995).
12. W. Shone et al., in: *ASSL'97*, Laser Zentrum Hannover, Germany, p. 292.
13. G. Hollemann, H. Muller, and H. Voelckel, *Proc. SPIE*, **2772**, 2–6 (1997).
14. A. A. Kaminskii, *Laser Crystals* [in Russian], Moscow (1975).
15. T. Kojima and K. Yasui, *Appl. Opt.*, **36**, 4981–4983 (1997).
16. S. Konno, S. Fujicawa, and K. Yasui, *Appl. Phys. Lett.*, **70**, 2650–2651 (1997).